Journal of Alloys and Compounds, 185 (1992) 99–107
JALCOM 222

Crystallographic data and magnetic properties of RT_6Ge_6 compounds (R≡Sc, Y, Nd, Sm, Gd–Lu; T≡Mn, Fe)

G. Venturini, R. Welter and B. Malaman
Laboratoire de Chimie du Solide Minéral, Associé au CNRS No. 158, Université de Nancy, I, B.P. 239, 54506, Vandoeuvre les Nancy Cedex (France)

(Received December 12, 1991)

Abstract

The iron and manganese germanides RT_6Ge_6 (R≡Sc, Y, Nd, Sm, Gd–Lu; T≡Mn, Fe) have been investigated by X-ray diffraction and susceptibility measurements in the temperature range 90–900 K. They crystallize in the known $HfFe_6Ge_6$, YCo_6Ge_6, $TbFe_6Sn_6$ or $HoFe_6Sn_6$ type of structure except $GdFe_6Ge_6$ which is of a new type. All the compounds are anti-ferromagnetic except the RMn_6Ge_6 (R≡Nd, Sm, Gd) compounds which behave ferrimagnetically. Weak coercive fields (down to 1 kOe) are measured in RMn_6Ge_6 (R≡Nd, Sm).

1. Introduction

Previous studies on RMn_6Sn_6 compounds have shown the interesting magnetic properties of this class of material [1, 2]. Some of them exhibit large coercive fields but the ordering temperature of these ferrimagnetic compounds remains rather weak. In another way, a crystallographic study on RFe_6Sn_6 [3] compounds allowed us to point out the occurrence of a long-range ordering in these compounds which was previously reported as isotypic of disordered YCo_6Ge_6-type structure [4]. Up to now, the corresponding manganese and iron germanides respectively have not been or have been partially studied [5, 6]. In order to enhance the transition temperatures, we have investigated these systems.

2. Experimental details

The compounds were synthesized from stoichiometric amounts of the elements. The mixture was compacted in a steel die and sealed in a silica tube under argon. They were then heated for 2 weeks at 1173 K for the iron compounds and 1073 K for the manganese compounds, except for samarium and neodymium compounds which were annealed at lower temperature (973 K). The purity of the samples was checked by X-ray analysis (Guinier Cu Kα, and curved detector INEL CPS 120 Co Kα). The parameters

0925-8388/92/$5.00
© 1992 – Elsevier Sequoia. All rights reserved

were refined by a least-squares procedure. Magnetic measurements were carried out on a Faraday balance in the temperature range 80–850 K and under fields up to 1.5 T.

3. Results

3.1. Crystallographic data

3.1.1. Manganese compounds

Twelve new germanides have been characterized: E≡Sc, Y, Nd, Sm, Gd–Lu. The crystallographic features of these compounds are summarized in Table 1. Scandium, yttrium and the heavier rare earth element compounds crystallize in the $HfFe_6Ge_6$-type structure [7] while neodymium and samarium (*i.e.* the larger rare earth elements) compounds crystallize in the YCo_6Ge_6 structure. It is worth noting that the series of the manganese germanides is longer than that of manganese stannides since $NdMn_6Ge_6$ is stable whereas $NdMn_6Sn_6$ does not exist. Such a result is apparently surprising since generally the replacement of germanium with tin shifts the stability range of a given structural type towards the larger rare earth elements. This behaviour is probably due to close Sn–Sn contacts as we have previously remarked in the refinements of $ScMn_6Sn_6$ and $TbMn_6Sn_6$ [8]. According to the variation of the cell volumes, in $YbMn_6Ge_6$, ytterbium seems to be in the III+ valence state.

3.1.2. Iron compounds

Ten iron germanides have been characterized: R≡Sc, Y, Gd–Lu. The cell parameters, space groups and structure type of these compounds are summarized in Table 2. The $YbFe_6Ge_6$ cell does not exhibit any volume anomaly. The smaller rare earth elements (scandium, ytterbium, lutetium)

TABLE 1

Cell parameters and structure types of RMn_6Ge_6 (R≡Sc, Y, Nd, Sm, Gd–Lu)[a]

Compound	a (Å)	c (Å)	V (Å^3)	Type
$ScMn_6Ge_6$	5.177(6)	8.084(4)	187.6	$HfFe_6Ge_6$
YMn_6Ge_6	5.233(2)	8.153(3)	193.4	$HfFe_6Ge_6$
$NdMn_6Ge_6$	5.258(1)	8.208(1)	196.5	YCo_6Ge_6
$SmMn_6Ge_6$	5.245(2)	8.187(2)	195.0	YCo_6Ge_6
$GdMn_6Ge_6$	5.242(2)	8.184(3)	194.8	$HfFe_6Ge_6$
$TbMn_6Ge_6$	5.232(1)	8.169(2)	193.7	$HfFe_6Ge_6$
$DyMn_6Ge_6$	5.228(1)	8.163(2)	193.2	$HfFe_6Ge_6$
$HoMn_6Ge_6$	5.230(1)	8.155(2)	193.2	$HfFe_6Ge_6$
$ErMn_6Ge_6$	5.221(2)	8.142(3)	192.2	$HfFe_6Ge_6$
$TmMn_6Ge_6$	5.219(1)	8.139(1)	191.9	$HfFe_6Ge_6$
$YbMn_6Ge_6$	5.212(1)	8.132(1)	191.3	$HfFe_6Ge_6$
$LuMn_6Ge_6$	5.211(1)	8.134(3)	191.3	$HfFe_6Ge_6$

[a]Space group, *P6/mmm*.

TABLE 2

Cell parameters and structure types of RFe_6Ge_6 (R≡Sc, Y, Gd–Lu)

Compound	a (Å)	b (Å)	c (Å)	V (Å^3(f.u.)$^{-1}$)	Space group	Type
$ScFe_6Ge_6$	5.087(1)	–	8.079(2)	181.02	*P6/mmm*	$HfFe_6Ge_6$
YFe_6Ge_6	8.116(2)	17.672(2)	5.120(2)	183.57	*Cmcm*	$TbFe_6Sn_6$
$GdFe_6Ge_6$	61.43(2)	8.137(2)	79.79(2)	184.63	*Pnma*	$GdFe_6Ge_6$
$TbFe_6Ge_6$	8.126(7)	17.76(2)	5.125(4)	184.82	*Cmcm*	$TbFe_6Sn_6$
$DyFe_6Ge_6$	8.118(2)	17.68(1)	5.116(2)	183.53	*Cmcm*	$TbFe_6Sn_6$
$HoFe_6Ge_6$	8.111(3)	17.66(2)	5.116(3)	183.19	*Cmcm*	$TbFe_6Sn_6$
$ErFe_6Ge_6$	8.103(2)	26.52(3)	5.108(3)	182.95	*Immm*	$HoFe_6Sn_6$
$TmFe_6Ge_6$	8.095(2)	26.53(1)	5.107(1)	182.82	*Immm*	$HoFe_6Sn_6$
$YbFe_6Ge_6$	5.097(1)	–	8.092(2)	182.09	*P6/mmm*	$HfFe_6Ge_6$
$LuFe_6Ge_6$	5.096(1)	–	8.081(2)	181.77	*P6/mmm*	$HfFe_6Ge_6$

f.u., formula unit.

compounds crystallize in the $HfFe_6Ge_6$–type structure, RFe_6Ge_6 (R≡Tm, Er) in the $HoFe_6Sn_6$ structure [3] and RFe_6Ge_6 (R≡Y, Tb, Dy, Ho) in the $TbFe_6Sn_6$ structure [3].

The case of $GdFe_6Ge_6$ is more complex since it exhibits additional superstructure lines in its X-ray diffraction pattern (Fig. 1(a)). We therefore may propose cell parameters and a space group allowing the indexation of the superstructure lines following the scheme given in Fig. 1(b). A first splitting of the $HfFe_6Ge_6$ superstructure lines into satellites, with a wavevector $\mathbf{Q}=(0, q, 0)$ in the orthohexagonal setting $(a, 3^{1/2}a, c)$, yields the types encountered in the corresponding stannides [3]. A second splitting of these first satellites, with a wavevector $\mathbf{R}=(r, 0, 0)$, leads to additional lines around these. The Bragg angles of the observed different lines lead to $q=0.867$ and $r=0.555$ and then to the cell parameters $a'=12a_H$, $b'=c_H$, $c'=9\times3^{1/2}a_H$ with space group *Pnma*.

The refinement of the atomic positions is under way.

3.2. Magnetic properties

3.2.1. Manganese compounds

The thermomagnetic properties of these compounds are collected in Table 3.

3.2.1.1. Paramagnetic state. The inverse susceptibility variation of scandium, yttrium, neodymium, samarium, ytterbium and lutetium compounds obeys a Curie–Weiss law. The paramagnetic Curie temperatures are rather high and characteristic of strong ferromagnetic couplings. The inverse susceptibility variation of the other compounds does not follow a Curie–Weiss law, at least in the studied temperature range. It exhibits a curvature, sometimes strong, whose concavity is directed towards the high temperature axis. This variation may be described with the hyperbolic form characteristic of

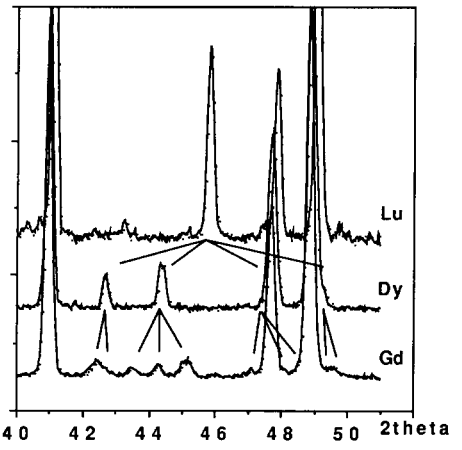

(a)

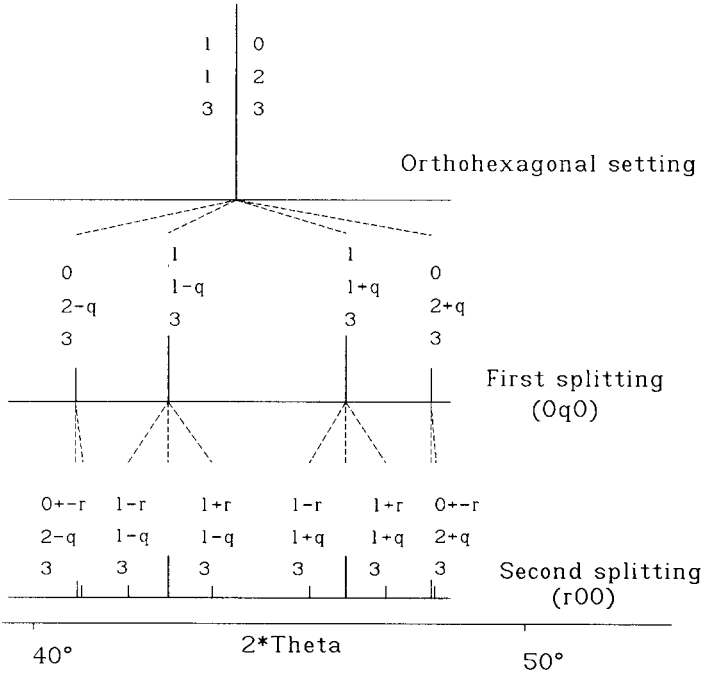

(b)

Fig. 1. (a) Partial X-ray diffraction pattern of $LuFe_6Ge_6$, $DyFe_6Ge_6$ and $GdFe_6Ge_6$. (b) Splitting scheme for the indexation transformation from hexagonal $HfFe_6Ge_6$-type structure to $GdFe_6Ge_6$ structure (for clarity the Miller indices are given vertically).

ferrimagnetic compounds [9]

$$\frac{1}{\chi} = \frac{T+\theta_p}{C} - \frac{\gamma}{T-\theta}$$

TABLE 3

Magnetic data for RMn_6Ge_6 (R≡Sc, Y, Nd, Sm, Gd–Lu)

Compound	T_N (K)	T_C (K)	θ_p (K)	μ_{eff} (μ_B)	μ_{Mn} (μ_B)[a]
$ScMn_6Ge_6$	516	–	500	7.48	3.05
YMn_6Ge_6	473	–	483	7.35	3.00
$NdMn_6Ge_6$	–	417	418	8.55	3.16
$SmMn_6Ge_6$	–	441	439	7.62	3.09
$GdMn_6Ge_6$	–	463	NCW[b]	–	
$TbMn_6Ge_6$	427	–	NCW	–	
$DyMn_6Ge_6$	423	–	NCW	–	
$HoMn_6Ge_6$	466	–	NCW	–	
$ErMn_6Ge_6$	475	–	NCW	–	
$TmMn_6Ge_6$	482	–	NCW	–	
$YbMn_6Ge_6$	480	–	449	8.14	2.75
$LuMn_6Ge_6$	509	–	485	7.35	3.00

[a] μ_{Mn} (μ_B) = $\frac{1}{6}(\mu_{eff}^2 - \mu_R^2)^{1/2}$.
[b] NCW, non-Curie–Weiss.

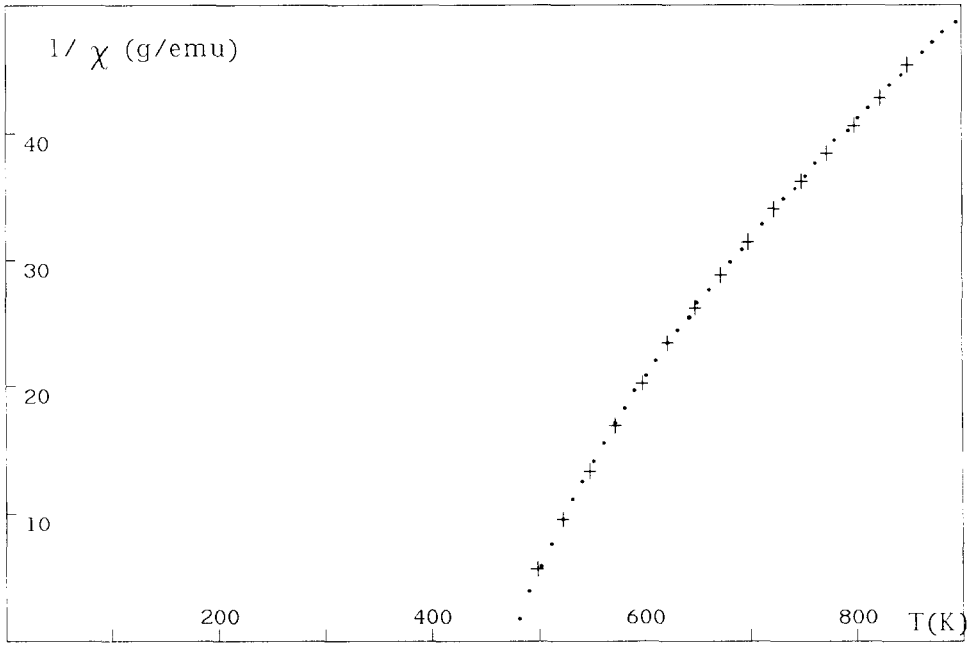

Fig. 2. Temperature dependence of the inverse susceptibility of $GdMn_6Ge_6$: +, experimental; ···, calculated.

Attempts to fit the parameters gave unsatisfactory results except for $GdMn_6Ge_6$ which is the compound exhibiting the largest curvature. In the other cases, owing to the shortness of the experimental temperature range and to the smaller curvatures, there are strong correlations between θ and γ, yielding unrealistic Curie constants. Figure 2 gives the experimental and

calculated inverse susceptibility for $GdMn_6Ge_6$. The fitted parameters are: $C=14.82$ ($\mu_{eff}=10.89$ μ_B), $\theta_p=46$ K, $\theta=302$ K and $\gamma=4979$.

The calculation of the paramagnetic manganese moment, assuming $\mu_{Gd}=7.94$ μ_B, gives $\mu_{Mn}=3.04$ μ_B which is in good agreement with the calculated values obtained with the Curie–Weiss-like compounds (Table 3). The low paramagnetic temperature θ_p indicates strong additional anti-ferromagnetic interactions.

3.2.1.2. Ordering state. Three types of magnetic ordering are encountered, as follows.

The lighter rare earth element compounds (neodymium, samarium, gadolinium) exhibit spontaneous magnetizations. The thermal variation of the susceptibility is typical of a P curve in the Néel classification for the ferrimagnetic compounds [10] (Fig. 3). The value of the magnetization which almost reaches saturation under an applied field of 1.5 T allows us to calculate the approximate manganese moment under the hypothesis of ferrimagnetic ordering: assuming a fully ordered rare earth moment at 90 K, the manganese moments are close to 2 μ_B (Table 4). Hysteresis effects are observed for the neodymium and samarium compounds, the coercive fields remaining rather weak at 90 K (Table 4).

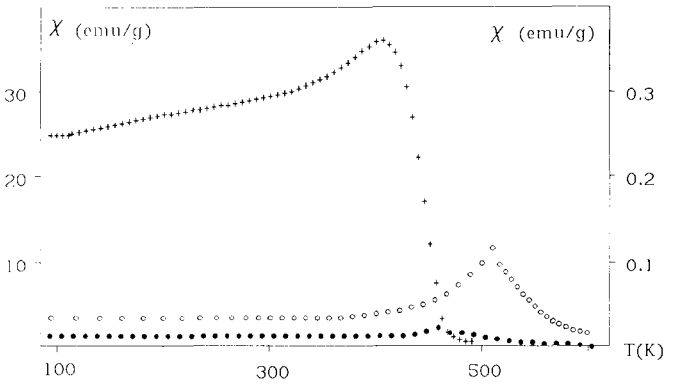

Fig. 3. Thermal variation of the susceptibility: +, $NdMn_6Ge_6$ ($H=0.05$ T, left-hand scale); ○, $LuMn_6Ge_6$ ($H=0.8$ T, right-hand scale); ●, $LuFe_6Ge_6$ ($H=0.8$ T, right-hand scale).

TABLE 4

Magnetization values of RMn_6Ge_6 (R≡Nd, Sm, Gd) at 300 and 90 K[a]

Compound	σ_s (300 K) (μ_B)	σ_s (90 K) (μ_B)	H_c (kOe)	gJ (μ_B)	μ_{Mn} (μ_B)
$NdMn_6Ge_6$	8.9	8.1	0.6	3.28	2.01
$SmMn_6Ge_6$	9.1	11.4	0.3	0.72	2.02
$GdMn_6Ge_6$	4.8	4.6	0.0	7.00	1.93

[a]H=1.5 T; calculated manganese moment values μ_{Mn} (μ_B)=$\frac{1}{6}$[σ_s (90 K)+gJ].

The paramagnetic rare earth (dysprosium to ytterbium) and diamagnetic rare earth elements (scandium, yttrium, lutetium) compounds are anti-ferromagnetic. All exhibit a rather sharp Néel point (Fig. 3) and a linear variation of the magnetization in the whole range of temperature and applied field. Down to 90 K there is no evidence of any ordering of the rare earth sublattice.

The terbium compound has an intermediate behaviour since it presents a metamagnetic transition under fairly or very strong applied fields as a function of the temperature (Fig. 4).

3.2.2. Iron compounds

The thermomagnetic properties of these compounds are summarized in Table 5. They are anti-ferromagnetic and their Néel points are strongly smoothed compared with the corresponding manganese compounds (Fig. 3). The inverse susceptibility curves do not exhibit a pronounced curvature as

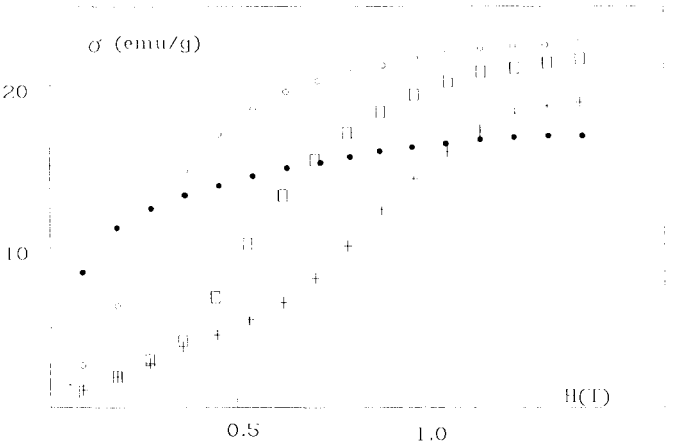

Fig. 4. Magnetization curves for $TbMn_6Ge_6$ at 300 K (+), 323 K (□), 373 K (○) and 423 K (●).

TABLE 5

Magnetic data for RFe_6Ge_6 (R≡Sc, Y, Gd–Lu)

Compound	T_N (K)	θ_p (K)	μ_{eff} (μ_B)
$ScFe_6Ge_6$	473	159	8.02
YFe_6Ge_6	477	108	7.82
$GdFe_6Ge_6$	482	5	11.39
$TbFe_6Ge_6$	480	5	12.71
$DyFe_6Ge_6$	475	62	13.17
$HoFe_6Ge_6$	473	45	13.34
$ErFe_6Ge_6$	470	105	12.07
$TmFe_6Ge_6$	465	121	10.74
$YbFe_6Ge_6$	475	103	8.84
$LuFe_6Ge_6$	452	112	7.65

in the manganese compounds and the paramagnetic Curie temperatures are much lower, involving stronger anti-ferromagnetic interactions. Down to 90 K there is no evidence of any ordering of the rare earth sublattice.

4. Discussion

The magnetic properties of RT_6Ge_6 (T≡Mn, Fe) exhibit a great variety of behaviours which can be discussed on the basis of our knowledge of related compounds and their magnetic structures. The binary compounds FeSn and FeGe B35 are built of ferromagnetic Fe(001) planes anti-ferromagnetically coupled to each other [11, 12]. Thus, assuming that in RFe_6Ge_6 compounds the iron sublattice keeps the same magnetic ordering, this implies a zero molecular field on the rare earth sublattice which will not favour its magnetic ordering.

The binary compounds MnGe and MnSn do not occur but there are reports of magnetic structures of several RMn_6Sn_6 compounds [2, 13]. Within the diamagnetic rare earth compounds, which are not perturbed by the magnetism of the rare earth element, preliminary studies [13] show that YMn_6Sn_6 and $ScMn_6Sn_6$ are complex helical structures built on ferromagnetic Mn(001) planes rotating over various angles along [001], and that $LuMn_6Sn_6$ is collinear anti-ferromagnetic built on the same ferromagnetic planes with the following stacking sequence along c: + + − − + + − −. Thus these compounds involve additional interplane ferromagnetic couplings which would explain the enhancement of the paramagnetic Curie temperature in the manganese compounds. Moreover, the occurrence of helical structures yields non-zero molecular fields on the rare earth sublattice which, through the polarization of the rare earth sublattice moments, will favour its magnetic ordering.

There are nevertheless some differences between the magnetic behaviours of the RMn_6Ge_6 and RMn_6Sn_6 compounds. First, as expected, the ordering temperature of the germanides with non-magnetic rare earth components are higher than those of the corresponding stannides, the ordering temperature decreasing with increasing size of the rare earth element. This behaviour comes from stronger Mn–Mn couplings due to shorter Mn–Mn interatomic distances. Another interesting difference is the evolution of the ordering temperature with the substitution of a magnetic rare earth element for a non-magnetic one: the substitution of gadolinium for lutetium enhances the ordering temperature of the stannides (T_N(Lu) = 353 K, T_C(Gd) = 435 K) whereas it acts in the opposite way for the germanides (T_N(Lu) = 509 K, T_C(Gd) = 463 K). This fact can be understood by considering an anti-ferromagnetic coupling between adjacent manganese planes surrounding the rare earth plane. In this case, both negative Mn–Mn and R–Mn interplane exchanges lead to a frustrated situation. Their relative strengths may explain the difference between the behaviours of the stannides and germanides. In the germanides, the shorter Mn–Mn interplane distances yield stronger Mn–Mn

couplings which are not fully compensated by the R–Mn couplings when the ferrimagnetic order takes place. The result is a lower number of ferrimagnetic compounds in the germanides.

A last remark relates to the occurrence of ferrimagnetic order in $SmMn_6Ge_6$ and $NdMn_6Ge_6$. It could come from strong Sm(Nd)–Mn couplings but this effect does not appear in the inverse susceptibility variations which closely follow Curie–Weiss behaviour. At this stage, we have to point out that samarium and neodymium are the largest rare earth elements in this series and that both compounds are isotypic with YCo_6Ge_6. Thus their behaviour may come either from the weakening of the Mn–Mn interplane couplings due to larger Mn–Mn distances or from a change in the interplane magnetic interactions due to the formation of corrugated manganese planes in this disordered structure.

5. Conclusion

This study brings new information and questions about the magnetic properties of RT_6X_6 compounds. Further investigations will require low temperature magnetic measurements and neutron diffraction studies. It would also be interesting to look for other compounds YCo_6Ge_6-type structure by alloying appropriate elements. Such experiments are under way.

References

1 G. Venturini, B. Chafik el Idrissi and B. Malaman, *J. Magn. Magn. Mater.*, *94* (1991) 349.
2 G. Venturini, B. Chafik el Idrissi, B. Malaman and D. Fruchart, *J. Less-Common Met.*, *174* (1991) 143.
3 G. Venturini, B. Chafik el Idrissi and B. Malaman, *Mater. Res. Bull.*, *26* (1991) 1331.
4 O. E. Koretskaia and R. V. Skolozdra, *Inorg. Mater. (USSR), Engl. Edn.*, *22* (1986) 606.
5 W. Bucholz and H. U. Schuster, *Z. Anorg. Allg. Chem.*, *482* (1981) 40.
6 B. Chabot and E. Parthé, *J. Less-Common Met.*, *96* (1983) L9.
7 R. R. Olenitch, L. G. Akselrud and Ya. P. Yarmoliuk, *Dopov. Akad. Nauk. Ukr. RSR, Ser. A*(2) (1981) 84.
8 G. Venturini, B. Chafik el Idrissi and B. Malaman, *Mater. Res. Bull.*, *26* (1991) 431.
9 A. Herpin, *Théorie du Magnétisme*, Bibliothèque des Sciences et Techniques Nucléaires, Presses Universitaire de France, Paris, 1968.
10 L. Néel, *Ann. Phys.*, *3* (1948) 137.
11 H. Watanabe and N. Kunitomi, *J. Phys. Soc. Jpn.*, *21* (1966) 10, 1932.
12 K. Yamaguchi and H. Watanabe, *J. Phys. Soc. Jpn.*, *22* (1967) 5, 1210.
13 G. Venturini *et al.*, *J. Alloys Comp.*, in the press.